

## Coordination Chemistry

## High-Spin Imido Cobalt Complexes with Imidyl Radical Character\*\*

Alexander Reckziegel, Manjinder Kour, Beatrice Battistella, Stefan Mebs, Katrin Beuthert, Robert Berger, and C. Gunnar Werncke\*

**Abstract:** We report on the synthesis of a variety of trigonal imido cobalt complexes  $[\text{Co}(\text{NAryl})\text{L}_2]^-$ , ( $\text{L} = \text{N}(\text{Dipp})\text{SiMe}_3$ ,  $\text{Dipp} = 2,6\text{-diisopropylphenyl}$ ) with very long  $\text{Co}-\text{N}_{\text{Aryl}}$  bonds of around 1.75 Å. Their electronic structure was interrogated using a variety of physical and spectroscopic methods such as EPR or X-Ray absorption spectroscopy which leads to their description as highly unusual imidyl cobalt complexes. Computational analyses corroborate these findings and further reveal that the high-spin state is responsible for the imidyl character. Exchange of the Dipp substituent on the imide by the smaller mesityl function (2,4,6-trimethylphenyl) effectuates the unexpected  $\text{Me}_3\text{Si}$  shift from the ancillary ligand set to the imidyl nitrogen, revealing a highly reactive, nucleophilic character of the imidyl unit.

Late 3d transition-metal imido complexes are of fundamental interest in coordination chemistry, as the metal-bound nitrene unit  $[\text{NR}]$  can be potentially transferred to unreactive substrates. This is increasingly employed for the catalytic amination of unfunctionalized C–H bonds or the aziridation of olefines.<sup>[1–12]</sup> Despite the resulting high demand for understanding late 3d-transition metal imido species, comprehensive knowledge about the electronic and structural factors that contribute to their properties and bond activation

How to cite: *Angew. Chem. Int. Ed.* **2021**, *60*, 15376–15380  
International Edition: doi.org/10.1002/anie.202103841  
German Edition: doi.org/10.1002/ange.202103841

reactivity is still lacking. Whereas most isolable imido metal complexes are found in a low-spin state, those with higher spin-states tend to be more reactive.<sup>[13–52]</sup>

In recent years substantial advances were made concerning more unusual bond situations of the  $[\text{MNR}]$  unit in higher spin states via structural and spectroscopic identification of singular examples of iron<sup>[28]</sup> and nickel imidyl complexes (also referred to as metal iminyl species)<sup>[29]</sup> or a nitrene copper compound<sup>[32]</sup> (Figure 1) using ancillary weak field ligands.

Herein we report on the synthesis of trigonal arylimido cobalt complexes, which contain very long  $\text{Co}-\text{N}_{\text{imide}}$  bonds of 1.75 Å. The use of a variety of analytical techniques reveals these compounds are best described as high-spin imidyl complexes, unprecedented for cobalt. Computational analyses corroborate these findings and clearly show the spin-state-dependent imidyl/imide interplay with the high-spin state evoking the radical imidyl character. Reduction of steric demand of the imide substituent results in an unexpected intramolecular shift of a  $\text{Me}_3\text{Si}$  unit from a silylamide ligand and reveals a nucleophilic character of the imidyl nitrogen.

The linear cobalt(I) silylamides  $\text{K}[\text{18c6}][\text{CoL}_2]$ ,  $\text{K}[\text{18c6}][\text{1}]$ , ( $\text{L} = \text{N}(\text{Dipp})\text{SiMe}_3$ )<sup>[53]</sup> or its derivative  $\text{K}[\text{crypt.222}][\text{1}]$  that contain weak field silylamide ligands<sup>[30,53,54]</sup> and exhibit magnetically free cobalt(I) ion behavior were reacted with

[\*] A. Reckziegel, Dr. M. Kour, K. Beuthert, Prof. Dr. R. Berger, Dr. C. G. Werncke  
Department of Chemistry  
Philipps-University Marburg  
Hans-Meerwein-Strasse 4, 35032 Marburg (Germany)  
E-mail: gunnar.werncke@chemie.uni-marburg.de

B. Battistella  
Institute of Chemistry  
Humboldt-Universität zu Berlin  
Brook-Taylor-Strasse 2, 12489 Berlin (Germany)

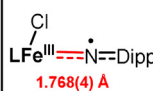
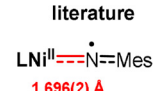
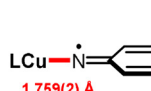
Dr. S. Mebs  
Department of Physics  
Freie Universität zu Berlin  
Arnimallee 14, 14195 Berlin (Germany)

[\*\*] A previous version of this manuscript has been deposited on a preprint server (<https://doi.org/10.26434/chemrxiv.14128709.v1>).

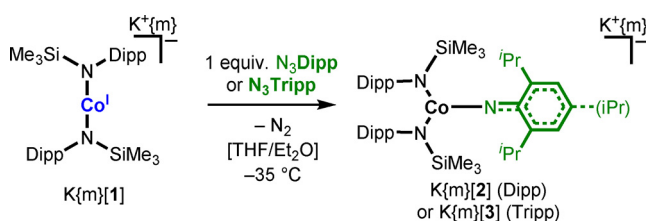
Supporting information (synthetic procedures, magnetic measurements, <sup>1</sup>H NMR, EPR, XANES/EXAFS spectra, computational details with xyz-coordinates, and crystallographic data) and the ORCID identification number(s) for the author(s) of this article can be found under:

<https://doi.org/10.1002/anie.202103841>.

© 2021 The Authors. Angewandte Chemie International Edition published by Wiley-VCH GmbH. This is an open access article under the terms of the Creative Commons Attribution Non-Commercial License, which permits use, distribution and reproduction in any medium, provided the original work is properly cited and is not used for commercial purposes.

Imide $[\text{NR}]^{2-}$	Imidyl $[\text{NR}]^-$	Nitrene $[\text{NR}]^0$
$\text{M}\equiv\text{N}-\text{R}$	$\text{M}=\ddot{\text{N}}-\text{R}$	$\text{M}-\ddot{\text{N}}-\text{R}$ (triplet)
or	or	or
$\text{M}=\ddot{\text{N}}-\text{R}$	$\text{M}-\ddot{\text{N}}-\text{R}$	$\text{M}-\ddot{\text{N}}-\text{R}$ (singlet)
literature		
		
1.768(4) Å	1.696(2) Å	1.759(2) Å
Fe <sup>III</sup> imidyl, <i>JACS</i> <b>2011</b>	Ni <sup>II</sup> imidyl, <i>Chem. Sci.</i> <b>2020</b>	Cu <sup>I</sup> triplet nitrene <i>Science</i> <b>2019</b>

**Figure 1.** Top: Simplified description of the different bonding modes of  $[\text{MNR}]$  units. Bottom: Bond lengths of known low-coordinated nitrene/imidyl complexes (Mes: 2,4,6-trimethylphenyl).



**Scheme 1.** Synthesis of  $\text{K}\{m\}[2]$  ( $m = \text{none}$ , crypt.222, 18c6) and  $\text{K}\{m\}[3]$  ( $m = \text{none}$ , 18c6) starting from  $\text{K}\{m\}[1]$  (Tripp = 2,4,6-triisopropylphenyl).

Dipp-N<sub>3</sub> or Tripp-N<sub>3</sub> (Scheme 1) at -35 °C in Et<sub>2</sub>O/THF. This resulted in an immediate color change from green to dark brown and concomitant N<sub>2</sub> evolution. Isolation yielded dark yellow crystals of K{m}[2] (Dipp; m=crypt, 18c6) K{crypt.222}[2] and K{18c6}[3] (Tripp). In solid state, the complex anions of all compounds exhibit similar structural metrics (Figure 2), for which the K{18c6}[2] is chosen as a representative for discussion. The complex anion shows a trigonally coordinated cobalt ion with a Co-N<sub>imide</sub> bond length of 1.751(2) Å. This is by at least 0.05 Å longer than in all other known aryl imido cobalt complexes (Co-N<sub>imide</sub> from 1.61 Å–1.70 Å).<sup>[13,14,16,23–25,34]</sup>

It resembles those of the known 3d-metal imidyl/nitrene compounds (Figure 1) and a matrix-isolated fluoronitroid cobalt species (Co-N 1.77 Å), for which imidyl/nitrene character was discussed.<sup>[12]</sup> Given these comparably long C-N<sub>imide</sub> bonds found for complexes [2]<sup>-</sup> and [3]<sup>-</sup> we were curious if this was connected to the unique anionic character of these imido complexes,<sup>[46]</sup> as nearly all comparable 3d-metal imido complexes are either neutral or cationic. Thus, the overall neutral cobalt(I) complex K[1]<sup>[55]</sup> was reacted with Dipp-N<sub>3</sub> and Tripp-N<sub>3</sub> which gave the respective complexes K[2] and K[3]. X-Ray analysis revealed (Figure 2) an

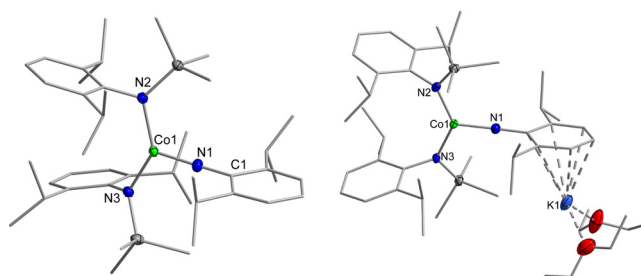


**Figure 2.** Molecular structure of K{18c6}[2] (left) and K[2] (right) in the solid state.<sup>[58]</sup> The K{18c6} cation, solvent molecules as well as H atoms are omitted for clarity. Selected bond lengths (Å) and angles (°): K{18c6}[2]: Co1-N1: 1.751(2); Co1-N2: 1.935(2); Co1-N3: 1.932(2); N1-C1: 1.347(2); Co1-N3-C31: 178.8(2); K[2]: Co1-N1 1.750(3); Co1-N2 1.916(2); Co1-N3 1.920(2); N1-C1 1.338(4); Co1-N1-C1 174.9(3).

intriguing direct potassium interaction, as cation coordination to imide metal units (such as Sc<sup>3+</sup>) is suggested as an important factor in modulating their properties, although direct structural evidence is lacking.<sup>[56,57]</sup> However, in the presented case no impact on the central arylimido cobalt unit was perceived (K[2]: Co-N<sub>imide</sub> 1.750(3) Å, K[3] Co-N<sub>imide</sub> 1.754(2) Å). Determination of the magnetic moment in solution by the Evans method gave  $\mu_{\text{eff}}=4.65 \mu_{\text{B}}$  (K{crypt.222}[2]) and  $\mu_{\text{eff}}=4.90 \mu_{\text{B}}$  (K{18c6}[2]). This is in approximate agreement with susceptibility measurements on K{18c6}[2] in solid state ( $\mu_{\text{eff}}=4.64 \mu_{\text{B}}$  at 300 K) revealing a linear  $1/\chi$  vs.  $T$  slope with no apparent spin-crossover (Figure 3a). The magnetic susceptibility at room temperature is higher than that of the related intermediate spin imido cobalt(III) complex [Co(N<sup>t</sup>Bu)(N(SiMe<sub>3</sub>)<sub>2</sub>)<sub>2</sub>]<sup>-</sup> (3.52  $\mu_{\text{B}}$ ),<sup>[30]</sup> (as well as of any other paramagnetic imido cobalt(III) complex<sup>[16,31,35]</sup>) and approaches the spin-only value of 4.92  $\mu_{\text{B}}$  of a quintet state. X-band EPR spectroscopy of K{18c6}[2] (d<sub>10</sub>-MeTHF, 8 K) gave decisive insights as it showed a broad signal at around  $g_1=5.0$  and a sharper signal at  $g_2=2.05$ , which is split due to the presence of hyperfine coupling (Figure 3b). These features could be modeled as a cobalt(II) ion bound to an organic radical anion (see Figure S27), where the high-field signal (Figure 3b, inset) represents the imide-based radical with moderate coupling to cobalt, the imide nitrogen and one hydrogen atom (presumably H<sub>para</sub>;  $A(^1\text{H})=6.8 \text{ G}$ ,  $A(^{59}\text{Co})=4.3 \text{ G}$ ,  $A(^{14}\text{N})=5.0 \text{ G}$ ). For more direct insight into the oxidation state of the metal, X-ray absorption spectroscopy (XAS) was employed (Figure 3c). For that we examined the pre-edge and edge regions of the Co 1s→3d\* transition of K{18c6}[2] as well as K[2] and the trigonal cobalt(II) amide K{crypt.222}[4] (high-spin Co<sup>II</sup>, synthesis see below) for comparison (solid state or frozen Me-THF solution). XANES shows similar edge positions for all compounds as well as a considerable pre-edge feature. In some cases a shoulder is observed in the edge rise, which, together with a shallow or even lacking edge maximum, is indicative of a low local coordination symmetry for all complexes. This is supported by EXAFS data which also gives congruent features in solid and solution state. Using cobalt oxides as references XANES suggests an oxidation

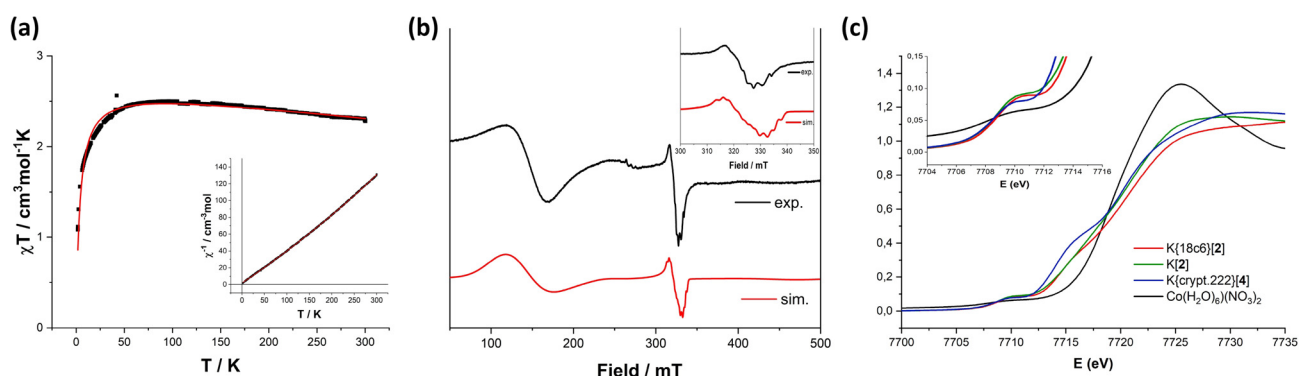


**Figure 3.** a) Variable-temperature susceptibility of K{18c6}[2] collected at 1 T, with  $\chi_{\text{M}}T=2.33 \text{ cm}^3 \text{ mol}^{-1} \text{ K}$  (300 K) and  $n_{\text{eff}}=4.635(4) \mu_{\text{B}}$ . Inset: Reciprocal molar magnetic susceptibility ( $\chi^{-1}$ ) for compound K{18c6}[2]. b) X-Band EPR spectra of K{18c6}[2] in frozen Me-THF solution at 8 K (black) and simulated spectrum (red). K{18c6}[2]:  $S_1=3/2$ ,  $g_{11}=5.0$ ,  $g_{12}=1.4$ ;  $S_2=1/2$ ,  $g_{21}=2.9$ ,  $g_{22}=2.05$ ,  $A_{22}(^1\text{H})=6.8 \text{ G}$ ,  $A_{22}(^14\text{N})=5.0 \text{ G}$ ,  $A_{22}(^{59}\text{Co})=4.3 \text{ G}$ . Hyperfine splitting for signal  $g_{22}=2.05$ . c) Solid-state X-ray absorption spectroscopy (XANES): K{18c6}[2] (red), K[2] (green), K{crypt.222}[4] (blue), Co<sup>II</sup> reference Co(H<sub>2</sub>O)<sub>6</sub>(NO<sub>3</sub>)<sub>2</sub> (black). Inset: Pre-K-edge absorption.

state of +2.0 for  $[2]^-$  (and  $K[2]$ ). This is only slightly higher than the corresponding cobalt(II) amide  $[4]^-$  (+1.7) and overall supports a non-innocent character of the imido/imidyl unit.

For further understanding of the experimental findings we turned to computational analysis of the seminal  $K\{18c6\}[2]$ . All electronic structures in their various possible spin states (high-, intermediate- and low-spin) were studied through dispersion-corrected density functional theory (DFT-D3) whereas various density functionals including the generalized gradient approximation (GGA) functionals BLYP and BP; hybrid functional B3-LYP; meta-hybrid functional M06; and the meta-GGA functional M06-L were used for determining the electronic energy differences between different spin states. For all functionals the high-spin state was found to be the most stable for  $[2]^-$  with the intermediate spin slightly higher in energy ( $7 \text{ kJ mol}^{-1}$  to  $38 \text{ kJ mol}^{-1}$ ) and an unfavored low-spin configuration ( $67 \text{ kJ mol}^{-1}$  to  $157 \text{ kJ mol}^{-1}$ ). The differences of the computed spin states of  $[2]^-$  are visualized best using the Co–N<sub>imide</sub> bond which is shortened significantly from 1.75 Å (high-spin), 1.72 Å (intermediate-spin) to 1.67 Å (low-spin; Table 1), whereas the high-spin case represents best the experimental structural features. The analysis of the bond order, a valuable tool for considering contributions made by occupied levels, gives for the high-spin configuration a Wiberg Bond Index (WBI) of 0.79 for the cobalt imidyl bond (Co1–N1), and thus reflects a single-bond character. When going to lower spin states the WBI successively increases (intermediate spin: 1.02, low spin: 1.48) and, together with the shortening of the Co–N<sub>imide</sub> bonds, leads to a more double-bond character. The N–C<sub>aryl</sub> bond lengths, sometimes used as an indicator for the electronic structure of a metal-bound aryl imide,<sup>[28]</sup> are more or less unaffected by the spin state in the present case.

In comparison with the lower spin states, slightly higher Mulliken atomic charges on the cobalt ion in the high-spin state could be observed, which indicates a moderately decreased covalent character of the Co–N<sub>imide</sub> bond (Table 2). The spin density plot, obtained from population analysis of high-spin  $[2]^-$ , shows not only the involvement of the aryl imido unit but also further contributions from the ancillary ligand set (Figure 4, left). The SOMO is mainly localized on the cobalt atom as well as on the imide nitrogen (Figure 4, right). Additional unpaired spin density is found at the *ortho* and *para* positions of the aromatic ring, which reflects well the situation derived from EPR spectroscopy.

**Table 1:** Comparison of selected bond lengths and angles of  $[2]^-$  calculated at the level of DFT-D3/M06-L with the experimental values.<sup>[a]</sup>

Bond lengths [Å] and angles [°]	Experimental values	Calculated		
		h.s.	i.s.	l.s.
$r(\text{Co1-N1})$	1.751	1.758	1.723	1.673
$r(\text{Co1-N2})$	1.935	1.951	1.928	1.858
$r(\text{Co1-N3})$	1.932	1.954	1.924	1.977
$r(\text{N1-C1})$	1.347	1.332	1.337	1.352
$\alpha(\text{Co1-N1-C1})$	178.8	172.39	172.53	162.76

[a] h.s. = high-spin, i.s. = intermediate-spin, l.s. = low-spin.

**Table 2:** Mulliken atomic charges and spin densities on the selected atoms of complex  $[2]^-$  at the level of DFT-D3/M06-L.

Atom	Mulliken atomic charges (spin density)		
	h.s.	i.s.	l.s.
Co1	0.767 (2.620)	0.720 (1.975)	0.688
N1	−0.650 (0.814)	−0.657 (−0.029)	−0.649
N2	−0.963 (0.133)	−0.940 (0.086)	−0.905
N3	−0.968 (0.128)	−0.945 (0.065)	−0.923

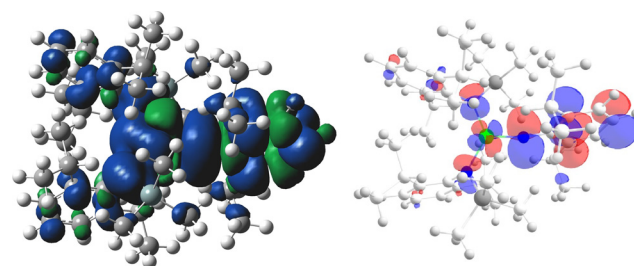
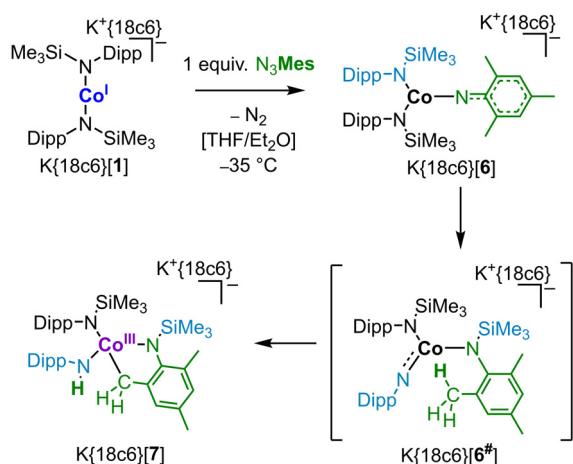


**Figure 4.** Left: Total spin density distribution of the complex  $[2]^-$  in high-spin state. An isosurface value of 0.003 a.u. is chosen. Right: SOMO of complex  $[2]^-$  (calculated with DFT-D3 using the density functional M06-L).

SOMO–1, SOMO–2, SOMO–3 and HOMO are of mixed character with unpaired spin density on the supporting aryl imido ligands as well (see SI). In comparison, for the intermediate-spin state the unpaired spin density is located almost exclusively on the cobalt ion (Table 2). Together with the increased WBI of 1.02 it gives the triplet state a distinct imide character. Overall, calculated electronic and structural parameters of high-spin  $[2]^-$  are in accord with the experimental findings and thus validate the description of  $[2]^-$  as an imidyl complex. This further shows that only in case of the high-spin state the imidyl radical character is present.

Having the first authenticated imidyl cobalt complexes in hand we examined their H atom abstraction capability. Reaction of  $K\{18c6\}[2]$  with 1,4-cyclohexadiene (1,4-CHD, BDE:  $76 \pm 2 \text{ kcal mol}^{-1}$ ) showed clean but slow formation of benzene and the cobalt(II) amide  $K\{18c6\}[\text{CoL}_2(\text{NHDipp})]$ ,  $K\{18c6\}[4]$ , which subsequently undergoes amide ligand scrambling to complex  $\{18c6\}[\text{CoL}(\text{NHDipp})_2]$ ,  $K\{18c6\}[5]$ . To reduce steric factors concerning the observed moderate reactivity of  $[2]^-$ , Mes–N<sub>3</sub> (Mes = 2,4,6-trimethylphenyl) was reacted with  $[1]^-$ . This gave the mesitylimido cobalt complex  $K\{18c6\}[2]$  (Scheme 2), which also has an enlarged Co–N<sub>imide</sub> bond (1.752(2) Å).  $K\{18c6\}[6]$  is highly reactive and could not be isolated in pure form as it facilitates intramolecular C–H bond activation of one of the Me<sub>iPr</sub> groups. It led to the alkyl/amido cobalt(III) complex  $K\{18c6\}[3]$ , which co-crystallized in varying ratios (Figure 5). Closer inspection of the molecular structure of  $K\{18c6\}[7]$  showed that the mesityl nitrogen is now carrying a Me<sub>3</sub>Si unit which originates from the –N(Dipp)SiMe<sub>3</sub> ligand set. This likely occurs starting from  $[6]^-$  with a Me<sub>3</sub>Si shift from the silylamide ligand to the mesityl





**Scheme 2.** Synthesis of  $[6]^-$  and formation of  $[7]^-$  by  $\text{Me}_3\text{Si}$ -group shift followed by intramolecular C–H activation by the transient cobalt Dipp imide  $[6]^-$ .

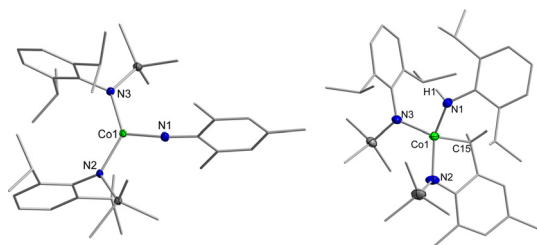


**Figure 5.** Molecular structure of  $\text{K}\{18\text{c}6\}[6]$  and  $\text{K}\{18\text{c}6\}[7]$  in the solid state.<sup>[58]</sup> The  $\text{K}\{18\text{c}6\}$  cation, solvent molecules as well as extraneous H atoms are omitted for clarity. Selected bond length (Å) and angles (°):  $\text{K}\{18\text{c}6\}[6]$ : Co1–N1 1.752(2); Co1–N2 1.931(1); Co1–N3 1.927(1); N1–C1 1.344(2); Co1–N1–C1 168.9(1);  $\text{K}\{18\text{c}6\}[7]$ : Co1–N1 1.897(3); Co1–N2 1.953(3); Co1–N3 1.977(3); Co1–C15 1.960(4).

imide unit which gives the transient cobalt complex  $[\text{CoL}(\text{NDipp})(\text{N}(\text{Mes})\text{SiMe}_3)]^-$  ( $[6]^-$ ). It points to a nucleophilic imide nitrogen in  $[6]^-$  that contrasts the general electrophilic behavior of late 3d-transition metal imides.<sup>[17,28,32,34,42–47]</sup>

Subsequently, intramolecular C–H bond activation in  $[6]^-$  leads to the highly labile organocobalt complex  $\text{K}\{18\text{c}6\}[7]$ . Intramolecular C–H bond activation is usually an unwanted phenomenon for late 3d-metal imido complexes and mainly occurs under insertion of the  $[\text{NR}]$  unit into a C–H bond of the imide substituent or the ancillary ligand set.<sup>[33,41]</sup> However, the formation of a metal–carbon bond was only observed for a mesityl imido cobalt(III) complex<sup>[16]</sup> and a transient aryl imido iron(II) complex.<sup>[36]</sup> There, a recombination of the formed carbon radical with the metal center and not the imide nitrogen was proposed. This is also plausible in the presented case, although a formal addition of the C–H bond along the Co–N unit or a deprotonation mechanism cannot be excluded. Overall, the experimental observations hint to a high reactivity of the imidyl cobalt(II) function and may explain its elusive character.<sup>[15,16,27,35]</sup>

We herein reported the synthesis and characterization of a variety of anionic and formally neutral trigonal arylimido cobalt complexes. They all exhibit by far the longest reported

Co–N<sub>imide</sub> bonds of around 1.75 Å. Comprehensive examination of the physical and spectroscopic properties led to their description as high-spin imidyl cobalt complexes. This is corroborated by computational analysis which connects the imidyl character to the complexes' high-spin state. With the smaller mesityl azide a mesitylimido cobalt complex was observed which underwent an unusual  $\text{Me}_3\text{Si}$ -group shift from the ancillary amide ligand set to the imidyl nitrogen. Overall, this study underscores the impact of the spin state on the central Co–N<sub>imide</sub> bond, and reveals a nucleophilic and highly reactive character of the cobalt imidyl unit.

## Acknowledgement

Funding by the Deutsche Forschungsgemeinschaft (DFG) is gratefully acknowledged: grant WE 5627/4-1 (C.G.W.). M.K. and R.B. thank the Center for Scientific Computing (CSC) Frankfurt for computer time and R. K. Bansal and M. Holthausen for discussion. Open access funding enabled and organized by Projekt DEAL.

## Conflict of interest

The authors declare no conflict of interest.

**Keywords:** C–H bond activation · cobalt · imido · quantum chemical calculations · spectroscopy

- [1] J. Y. Park, Y. Kim, D. Y. Bae, Y. H. Rhee, J. Park, *Organometallics* **2017**, *36*, 3471.
- [2] H. Lu, X. P. Zhang, *Chem. Soc. Rev.* **2011**, *40*, 1899.
- [3] F. Collet, R. H. Dodd, P. Dauban, *Chem. Commun.* **2009**, 5061.
- [4] V. Bagchi, A. Kalra, P. Das, P. Paraskevopoulou, S. Gorla, L. Ai, Q. Wang, S. Mohapatra, A. Choudhury, Z. Sun, T. R. Cundari, P. Stavropoulos, *ACS Catal.* **2018**, *8*, 9183.
- [5] P. F. Kuijpers, J. I. van der Vlugt, S. Schneider, B. de Bruin, *Chem. Eur. J.* **2017**, *23*, 13819.
- [6] D. N. Zalatan, J. Du Bois in *Metal-Catalyzed Oxidations of C–H to C–N Bonds*, 2009, (Eds.: JQ. Yu, Z. Shi), Springer, Berlin, Heidelberg, **2009**, pp. 347–378.
- [7] Y. Dong, C. J. Lund, G. J. Porter, R. M. Clarke, S.-L. Zheng, T. R. Cundari, T. A. Betley, *J. Am. Chem. Soc.* **2021**, *143*, 817.
- [8] R. Breslow, S. H. Gellman, *J. Am. Chem. Soc.* **1983**, *105*, 6728.
- [9] R. Breslow, S. H. Gellman, *J. Chem. Soc. Chem. Commun.* **1982**, 1400.
- [10] M. M. Díaz-Requejo, T. R. Belderráin, M. C. Nicasio, S. Trofimenko, P. J. Pérez, *J. Am. Chem. Soc.* **2003**, *125*, 12078.
- [11] D. Hazelard, P.-A. Nocquet, P. Compain, *Org. Chem. Front.* **2017**, *4*, 2500.
- [12] T. Stüker, T. Hohmann, H. Beckers, S. Riedel, *Angew. Chem. Int. Ed.* **2020**, *59*, 23174; *Angew. Chem.* **2020**, *132*, 23374.
- [13] T. A. Betley, J. C. Peters, *J. Am. Chem. Soc.* **2003**, *125*, 10782.
- [14] X. Hu, K. Meyer, *J. Am. Chem. Soc.* **2004**, *126*, 16322.
- [15] L. Zhang, Y. Liu, L. Deng, *J. Am. Chem. Soc.* **2014**, *136*, 15525.
- [16] E. R. King, G. T. Sazama, T. A. Betley, *J. Am. Chem. Soc.* **2012**, *134*, 17858.
- [17] J. Du, L. Wang, M. Xie, L. Deng, *Angew. Chem. Int. Ed.* **2015**, *54*, 12640; *Angew. Chem.* **2015**, *127*, 12831.
- [18] B. Wu, R. Hernández Sánchez, M. W. Bezpalko, B. M. Foxman, C. M. Thomas, *Inorg. Chem.* **2014**, *53*, 10021.

- [19] R. E. Cowley, R. P. Bontchev, J. Sorrell, O. Sarracino, Y. Feng, H. Wang, J. M. Smith, *J. Am. Chem. Soc.* **2007**, *129*, 2424.
- [20] Y. Liu, L. Deng, *J. Am. Chem. Soc.* **2017**, *139*, 1798.
- [21] J. J. Scepianiak, J. A. Young, R. P. Bontchev, J. M. Smith, *Angew. Chem. Int. Ed.* **2009**, *48*, 3158; *Angew. Chem.* **2009**, *121*, 3204.
- [22] D. T. Shay, G. P. A. Yap, L. N. Zakharov, A. L. Rheingold, K. H. Theopold, *Angew. Chem. Int. Ed.* **2006**, *45*, 7870; *Angew. Chem.* **2006**, *118*, 8034.
- [23] X. Dai, P. Kapoor, T. H. Warren, *J. Am. Chem. Soc.* **2004**, *126*, 4798.
- [24] D. M. Jenkins, T. A. Betley, J. C. Peters, *J. Am. Chem. Soc.* **2002**, *124*, 11238.
- [25] C. Jones, C. Schulten, R. P. Rose, A. Stasch, S. Aldridge, W. D. Woodul, K. S. Murray, B. Moubarak, M. Brynda, G. La Macchia, L. Gagliardi, *Angew. Chem. Int. Ed.* **2009**, *48*, 7406; *Angew. Chem.* **2009**, *121*, 7542.
- [26] M. P. Mehn, S. D. Brown, D. M. Jenkins, J. C. Peters, L. Que, *Inorg. Chem.* **2006**, *45*, 7417.
- [27] S. Thyagarajan, D. T. Shay, C. D. Incarvito, A. L. Rheingold, K. H. Theopold, *J. Am. Chem. Soc.* **2003**, *125*, 4440.
- [28] D. A. Iovan, T. A. Betley, *J. Am. Chem. Soc.* **2016**, *138*, 1983.
- [29] Y. Dong, J. T. Lukens, R. M. Clarke, S.-L. Zheng, K. M. Lancaster, T. A. Betley, *Chem. Sci.* **2020**, *123*, 4623.
- [30] A. Reckziegel, C. Pietzonka, F. Kraus, C. G. Werncke, *Angew. Chem. Int. Ed.* **2020**, *59*, 8527; *Angew. Chem.* **2020**, *132*, 8605.
- [31] Y. Baek, T. A. Betley, *J. Am. Chem. Soc.* **2019**, *141*, 7797.
- [32] K. M. Carsch, I. M. DiMucci, D. A. Iovan, A. Li, S.-L. Zheng, C. J. Titus, S. J. Lee, K. D. Irwin, D. Nordlund, K. M. Lancaster, T. A. Betley, *Science* **2019**, *365*, 1138.
- [33] Y. Baek, E. T. Hennessy, T. A. Betley, *J. Am. Chem. Soc.* **2019**, *42*, 16944.
- [34] Y. Liu, J. Du, L. Deng, *Inorg. Chem.* **2017**, *56*, 8278.
- [35] D. T. Shay, G. P. A. Yap, L. N. Zakharov, A. L. Rheingold, K. H. Theopold, *Angew. Chem. Int. Ed.* **2005**, *44*, 1508; *Angew. Chem.* **2005**, *117*, 1532.
- [36] J. Cheng, J. Liu, X. Leng, T. Lohmiller, A. Schnegg, E. Bill, S. Ye, L. Deng, *Inorg. Chem.* **2019**, *58*, 7634.
- [37] T. R. Cundari, *J. Am. Chem. Soc.* **1992**, *114*, 7879.
- [38] A. I. Olivos Suarez, V. Lyaskovskyy, J. N. H. Reek, J. I. van der Vlugt, B. de Bruin, *Angew. Chem. Int. Ed.* **2013**, *52*, 12510; *Angew. Chem.* **2013**, *125*, 12740.
- [39] K. Ray, F. Heims, F. F. Pfaff, *Eur. J. Inorg. Chem.* **2013**, 3784.
- [40] R. Eikey, *Coord. Chem. Rev.* **2003**, *243*, 83.
- [41] J. F. Berry, *Comments Inorg. Chem.* **2009**, *30*, 28.
- [42] E. R. King, E. T. Hennessy, T. A. Betley, *J. Am. Chem. Soc.* **2011**, *133*, 4917.
- [43] M. J. T. Wilding, D. A. Iovan, A. T. Wrobel, J. T. Lukens, S. N. MacMillan, K. M. Lancaster, T. A. Betley, *J. Am. Chem. Soc.* **2017**, *139*, 14757.
- [44] E. T. Hennessy, R. Y. Liu, D. A. Iovan, R. A. Duncan, T. A. Betley, *Chem. Sci.* **2014**, *5*, 1526.
- [45] E. Kogut, H. L. Wiencko, L. Zhang, D. E. Cordeau, T. H. Warren, *J. Am. Chem. Soc.* **2005**, *127*, 11248.
- [46] J. Xiao, L. Deng, *Dalton Trans.* **2013**, *42*, 5607.
- [47] C. A. Laskowski, A. J. M. Miller, G. L. Hillhouse, T. R. Cundari, *J. Am. Chem. Soc.* **2011**, *133*, 771.
- [48] L. N. Grant, M. E. Carroll, P. J. Carroll, D. J. Mindiola, *Inorg. Chem.* **2016**, *55*, 7997.
- [49] D. J. Mindiola, G. L. Hillhouse, *J. Am. Chem. Soc.* **2001**, *123*, 4623.
- [50] D. J. Mindiola, G. L. Hillhouse, *Chem. Commun.* **2002**, 1840.
- [51] R. Waterman, G. L. Hillhouse, *J. Am. Chem. Soc.* **2003**, *125*, 13350.
- [52] N. D. Harrold, G. L. Hillhouse, *Chem. Sci.* **2013**, *4*, 4011.
- [53] C.-Y. Lin, J. C. Fettinger, F. Grandjean, G. J. Long, P. P. Power, *Inorg. Chem.* **2014**, *53*, 9400.
- [54] C. G. Werncke, E. Suturina, P. C. Bunting, L. Vendier, J. R. Long, M. Atanasov, F. Neese, S. Sabo-Etienne, S. Bontemps, *Chem. Eur. J.* **2016**, *22*, 1668.
- [55] R. Weller, I. Müller, C. Duhayon, S. Sabo-Etienne, S. Bontemps, C. G. Werncke, *Dalton Trans.* **2021**, *50*, 4890.
- [56] S. Kundu, E. Miceli, E. Farquhar, F. F. Pfaff, U. Kuhlmann, P. Hildebrandt, B. Braun, C. Greco, K. Ray, *J. Am. Chem. Soc.* **2012**, *134*, 14710.
- [57] I. Monte-Pérez, S. Kundu, K. Ray, *Z. Anorg. Allg. Chem.* **2015**, *641*, 78.
- [58] Deposition Numbers 2056475 (K{crypt.222}[1]), 2056468 (K{18c6}[2]), 2056470 (K{crypt.222}[2]), 2056477 (K[2]), 2056474 (K{18c6}[3]), 2056465 (K[3]), 2056469 (K{18c6}[4]), 2056472 (K{crypt.222}[4]), 2056477 (K[4]), 2056471 (K{18c6}[5]), 2056473 (K{crypt.222}[5]), 2056476 (K{18c6}[6]), and 2056467 (K{18c6}[7]) contain the supplementary crystallographic data for this paper. These data are provided free of charge by the joint Cambridge Crystallographic Data Centre and Fachinformationszentrum Karlsruhe Access Structures service [www.ccdc.cam.ac.uk/structures](http://www.ccdc.cam.ac.uk/structures).

Manuscript received: March 17, 2021  
Revised manuscript received: May 10, 2021  
Accepted manuscript online: May 11, 2021  
Version of record online: June 9, 2021